Computational and Structural Biotechnology Journal 18 (2020) 1–8

COMPUTATIONAL AND STRUCTURAL BIOTECHNOLOGY JOURNAL

journal homepage: www.elsevier.com/locate/csbj

Optimizing cultivation of *Cordyceps militaris* for fast growth and cordycepin overproduction using rational design of synthetic media

Nachon Raethong [a], Hao Wang [b,c,d], Jens Nielsen [b,e], Wanwipa Vongsangnak [f,g,h,*]

[a] *Interdisciplinary Graduate Program in Bioscience, Faculty of Science, Kasetsart University, Bangkok, Thailand*
[b] *Department of Biology and Biological Engineering, Chalmers University of Technology, Gothenburg, Sweden*
[c] *Wallenberg Centre for Molecular and Translational Medicine, University of Gothenburg, Gothenburg, Sweden*
[d] *National Bioinformatics Infrastructure Sweden, Science for Life Laboratory, Chalmers University of Technology, Gothenburg, Sweden*
[e] *Novo Nordisk Foundation Center for Biosustainability, Technical University of Denmark, Lyngby, Denmark*
[f] *Department of Zoology, Faculty of Science, Kasetsart University, Bangkok, Thailand*
[g] *Omics Center for Agriculture, Bioresources, Food, and Health, Kasetsart University (OmiKU), Bangkok, Thailand*
[h] *Center for Systems Biology, School of Biology and Basic Medical Sciences, Soochow University, Suzhou, China*

ARTICLE INFO

Article history:
Received 28 August 2019
Received in revised form 1 November 2019
Accepted 8 November 2019
Available online 26 November 2019

Keywords:
Cordycepin
Cordyceps militaris
Genome-scale modeling
Synthetic media design
Systems biology

ABSTRACT

Cordyceps militaris is an entomopathogenic fungus which is often used in Asia as a traditional medicine developed from age-old wisdom. Presently, cordycepin from *C. militaris* is a great interest in medicinal applications. However, cellular growth of *C. militaris* and the association with cordycepin production remain poorly understood. To explore the metabolism of *C. militaris* as potential cell factories in medical and biotechnology applications, this study developed a high-quality genome-scale metabolic model of *C. militaris*, *i*NR1329, based on its genomic content and physiological data. The model included a total of 1329 genes, 1821 biochemical reactions, and 1171 metabolites among 4 different cellular compartments. Its *in silico* growth simulation results agreed well with experimental data on different carbon sources. *i*NR1329 was further used for optimizing the growth and cordycepin overproduction using a novel approach, POPCORN, for rational design of synthetic media. In addition to the high-quality GEM *i*NR1329, the presented POPCORN approach was successfully used to rationally design an optimal synthetic medium with C:N ratio of 8:1 for enhancing 3.5-fold increase in cordycepin production. This study thus provides a novel insight into *C. militaris* physiology and highlights a potential GEM-driven method for synthetic media design and metabolic engineering application. The *i*NR1329 and the POPCORN approach are available at the GitHub repository: https://github.com/sysbiomics/*Cordyceps_militaris*-GEM.

1. Introduction

Natural products from microbial communities of eukaryotic hosts play a major role in modern drug discovery [1,2]. It is often found in insect pathogenic fungi that are effective at overcoming insect immunities, for example it can secrete bioactive compounds e.g., destruxin, oosporein and cordycepin [3–6]. These compounds substantially display a broad range of biological activities against insect pests and human disease vectors, pathogenic bacteria and human disease like cancer [4–7]. Among them, cordycepin is an important bioactive compound isolated from the fungus *Cordyceps militaris*. It can be used as anticancer agent that mediates apoptotic signaling in various types of human cancers, such as ovarian [8] and lung [9]. Moreover, it was recently discovered to be a novel anti-adipogenic potential through the activation of AMP-activated protein kinase-dependent pathway which consequently induces metabolic reprogramming and browning in white adipose tissues [10]. Cordycepin has also found novel applications for both agrochemical and pharmaceutical sectors [11]. However, *C. militaris* naturally has slow growth in lepidopteran larvae. Hence, artificial cultures become more favorable solution for biotechnological production of *C. militaris* for high cordycepin yield. Previously, raw materials, such as rice, yeast extract, peptone have been used as the main components in the cultivation media of *C. militaris*, but growth is still slow and cordycepin production is low [3].

During the past decade, the complete genome of *C. militaris* has been sequenced at least three times using different sequencing technologies including Roche 454 [12] and PacBio RS II [13,14].

* Corresponding author at: Department of Zoology, Faculty of Science, Kasetsart University, Bangkok, Thailand.
E-mail address: wanwipa.v@ku.ac.th (W. Vongsangnak).

https://doi.org/10.1016/j.csbj.2019.11.003
2001-0370/

To date,more than 300 × coverage of the *C. militaris* genome has been obtained and assembled into the genome in size of 32.57 Mb [13]. In addition, the transcriptomic analysis of *C. militaris* in response to different carbon sources was recently studied and showed that up-regulation of the cordycepin biosynthetic associated genes were observed when *C. militaris* cultured in favorable source of carbon [15]. A more recent study also showed that the cultivation of *C. militaris* strains for growth and cordycepin production was rightly dependent on preferable carbon source [16]. This finding suggests that the systems design of cultivation medium is crucial for growth and cordycepin production. To design an optimal cultivation medium, reconstructing a genome-scale model (GEM) serves as a strategic approach because it allows to define growth requirements and further probe cellular metabolism and physiology under various cultivation conditions [17,18].

In the present work, we developed the most comprehensive GEM of *C. militaris* towards optimizing cultivation conditions of *C. militaris* for fast growth and cordycepin overproduction. Initially, a GEM of *C. militaris* was reconstructed based on genome sequences and physiological data. Biomass and additional important reactions were included based on the measurement data, biochemical databases and published literature. The GEM was subsequently used for simulation and validation by experimental data. In the end, GEM was subjected for optimizing fast growth and overproduction of cordycepin using our rational design of synthetic media. This study provides a system-level approach for enhancing *C. militaris* growth towards an efficient fungal cell factory for the overproduction of cordycepin and other bioactive compounds.

2. Material and methods

2.1. GEM reconstruction

The GEM was reconstructed by using the RAVEN toolbox version 2.0 [19]. The modeling process involved template GEMs preparation, draft creation, manual curation, parameter fitting and GEM validation. Initially, previous GEMs of closely related fungal species including *Penicillium chrysogenum* Wisconsin 54-1255 (*i*AL1006) [20], *Aspergillus nidulans* FGSC A4 (*i*HD666) [21], *Aspergillus oryzae* RIB40 (*i*WV1314) [22] and *Neurospora crassa* (*i*JDZ836) [23] were used as template models. To prevent the introduction of duplicated metabolites and reactions from various template models, their different identifiers were inspected and standardized for reconstruction, according to the major databases (e.g., MetaCyc [24] and KEGG [25]). Draft model of *C. militaris* was then generated based on protein orthology between the protein encoding sequences of template model species and the protein sequences of *C. militaris*. Orthologous proteins were obtained using bi-directional sequence alignment analysis using *getBlast* function, with E-value of 10^{-05}, identity of 40% and alignment length of 200 amino acids as cut-offs. These orthologous proteins were mapped to the template models using *getModelFromHomology* function. When integrating draft model of *C. militaris*, the template model from *i*AL1006 was used as a basis. The other templates from *i*WV1314, *i*HD666 and *i*JDZ836 as well as an earlier genome-scale metabolic network of *C. militaris* (*i*WV1170) [26] were used to enhance metabolic coverage through mapping Enzyme Commission (EC) numbers and orthologous proteins, which determined a list of new reactions that were subsequently added using *addGenesMetsRxns* function.

For determining biomass composition, dried mycelia of *C. militaris* grown on glucose cultivation were collected and subjected to estimate the proportions of carbohydrate, protein, lipid and other elements using proximate analysis followed by AOAC official methods of analysis and calculations. The individual compositions of each amino acid, monosaccharaide, free fatty acid, sphingolipid and sterol ester were obtained from previous studies of *Cordyceps* species [27]. The weights of each nucleotide in DNA and RNA of *C. militaris* were calculated based on the reported GC content of 51.40% [12] and 55.98% [15], respectively. The addition of biomass composition reactions, specific biochemical reactions and exchange reactions for both consumption and production of substrates and metabolites based on experimental measurements, biochemical text books and literature supports were performed through manual curation. Finally, the reconstructed GEM of *C. militaris* was examined according to community standard and followed by growth simulation that was carried out by RAVEN 2.0 [19] in MATLAB (R2016b) using Gurobi optimizer (Gurobi Optimization Inc., Houston, Texas) as linear programming solver. All scripts for model reconstruction and simulation of *C. militaris*, as well as the generated model files (.mat, .xml, .xlsx, .txt, .yml), are deposited into a public repository on GitHub (https://github.com/sysbiomics/*Cordyceps_militaris*-GEM).

2.2. Parameter fitting for physiological growth simulation and GEM validation

Biomass production was then set as the objective function for maximizing growth prediction in varying different constraints with flux balance analysis (FBA). For energy parameters, ATP maintenance reaction (m_{ATP}) was constrained with one mmol gDW^{-1}-h^{-1} according to earlier fungal models [20,22]. In addition to aerobic growth, the oxidative phosphorylation efficiency (P/O ratio) was set to be 2.5 according to the value used by the GEM of *A. oryzae*, *i*WV1314 and the GEM of *P. chrysogenum*, *i*AL1006. For ATP cost adjusting for *C. militaris* biomass synthesis (Y_{xATP}), thus the maximum specific growth rate (μ_{max}) obtained from glucose cultivation was therefore used for Y_{xATP} optimization with FBA. After fitting growth parameters, the GEM was then applied with FBA for physiological growth characterization. Quantitative comparisons of predictive and experimental growth rates were then performed for GEM validation.

2.3. Growth capability analysis underlying nutritional perturbation

Due to nutritional substrates that uptake from *in silico*, *in vitro* and *in vivo* media are mainly contributed to growth behavior and cellular metabolism. Therefore, we exploited the reconstructed GEM for determining growth capability of *C. militaris* underlying nutritional perturbations by the following two different levels. Level 1 was perturbation on carbon and nitrogen availabilities, as well as level 2 was perturbation on nutrient type variation. For level 1, we perturbed the availabilities of carbon and nitrogen into three different conditions including carbon limited condition (C-limited), nitrogen limited condition (N-limited) and CN-limited by constraining the uptake rates of ammonia and glucose. For example, under C-limited condition, one mmol $gDW^{-1}h^{-1}$ of ammonia was supplied for all growth simulations where glucose was limited to zero. In contrast to N-limited condition, one mmol $gDW^{-1}h^{-1}$ of glucose was supplied for all growth simulations while ammonia was limited to zero. Otherwise, both glucose and ammonia were limited to zero. Following level, nutrient variation was applied by one-at-a-time perturbation on the uptake rates of 133 nutrient types. In which, each nutrient type was uptake for one mmol $gDW^{-1}h^{-1}$ under C-limited and N-limited conditions. Otherwise, the uptake rates of any nutrients types were 2 mmol $gDW^{-1}h^{-1}$ under CN-limited condition. Thereafter growth simulation was carried out as detailed in a MATLAB script, name *final_mVaried.m*. The simulation growth behavior matrix between the perturbation on carbon and nitrogen availabilities (level 1, 3 condi-

tions) against nutrient variation (level 2, 133 nutrient types) was used to explore growth capability of *C. militaris* on different nutrients. For example, if the simulation growth behaviors showed that *C. militaris* could grow in all 3 perturbation conditions (i.e. C-limited, N-limited and CN-limited conditions) when nutrient type A was uptake. Nutrient type A could then be used as a complex of carbon and/or nitrogen source which was classified into Cluster 1. While if the simulation growth behaviors showed that *C. militaris* could grow in only N-limited condition when nutrient type B was uptake. Hereby, nutrient type B could then be used as a nitrogen source which was classified into Cluster 2. In contrast, if the simulation growth behaviors showed that *C. militaris* could grow in only C-limited when nutrient type C was uptake. Thereby, nutrient type C could then be used as a carbon source which was classified into Cluster 3. Otherwise, *C. militaris* could not utilize those nutrient types as sole carbon and/or nitrogen sources thus they were classified into Cluster 4.

2.4. Development of POPCORN as a constraint-based modeling approach to optimize the PrOPortion of CarbOn and nitRogeN

Growth behavior and cordycepin production are promising as the commercial requirements for *C. militaris*. However, the optimization of biomass and cordycepin production in *C. militaris* remains complex and depends on cellular growth behaviors, proportion of carbon and nitrogen sources as well as nutritional perturbations. We therefore applied FBA to solve the optimization problem between cellular growth, cordycepin production and the proportion of carbon and nitrogen sources in term of C:N ratio by developing a constraint-based modeling approach called POPCORN. This approach was implemented as the RAVEN 2.0 plug-in that generated a series of C:N ratios ranged from low to high and plug-in for GEM simulation with FBA. With these C:N ratios series, biomass production was maximized to obtain μ_{max}. After that, growth was fixed with the 0.9 of μ_{max}, then the production flux of cordycepin was maximized. The default coefficient used in POPCORN was set according to the same default coefficient implemented for Flux Scanning based on Enforced Objective Flux (FSEOF) [19]. By the end, the experimentation was further carried out to validate the POPCORN simulation result.

2.5. Growth physiology and cordycepin production of C. militaris grown in synthetic media

The *C. militaris* strain used in this study was TBRC6039. The stock culture was maintained as frozen hyphal suspension in 10% (v/v) glycerol at −80 °C [28]. For inoculum preparation, 0.5 mL of the stock solution was added in a 250-mL shake flask containing 75 mL of yeast extract-peptone-dextrose medium, and the cultivation was grown at 22 °C with shaking of 250 rpm for 7 days without light induction. For the cultivation, 5% (v/v) of *C. militaris* inoculum was transferred into individual sterile 250-mL jars containing 75 mL of cultivation medium enclosed with a sterile filter cap. The synthetic media used for GEM validation were composed of 0.5 g L^{-1} $MgSO_4{\cdot}7H_2O$, 0.5 g L^{-1} $K_2HPO_4{\cdot}3H_2O$, 0.5 g L^{-1} KH_2PO_4, 0.1 g L^{-1} $CaCl_2$, 0.1 g L^{-1} $FeSO_4{\cdot}7H_2O$, 40 m mol L^{-1} $(NH_4)_2SO_4$ and 20 g L^{-1} of carbon source (i.e. glucose, fructose, arabinose, xylose or sucrose). In addition to cultivation series for POPCORN verification, the rational synthetic media were prepared in the same manner which composed of 0.5 g L^{-1} $MgSO_4{\cdot}7H_2O$, 0.5 g L^{-1} $K_2HPO_4{\cdot}3H_2O$, 0.5 g L^{-1} KH_2PO_4, 0.1 g L^{-1} $CaCl_2$, 0.1 g L^{-1} $FeSO_4{\cdot}7H_2O$, but the compositions of $(NH_4)_2SO_4$ and glucose were varied according to Table S1. All cultivations were performed in batch mode at 22 °C under static condition without light induction. All experiments were independently conducted in three biological replicates. For dry weight (DW) determination, mycelia were harvested through a filter paper, washed at least three times with distilled water and then dried using freeze dryer at −110 °C until a constant weight was obtained and calculated for the μ_{max}. The cultivation broth was used to measure the concentrations of residual sugars and cordycepin by high performance liquid chromatography (HPLC). To determine the concentration of residual sugars by HPLC (Thermo Scientific, USA), 5 mmol L^{-1} H_2SO_4 was used as the mobile phase with a flow rate of 0.6 mL min^{-1} on Aminex HPX-87H column (300 mm × 7.8 mm) at 60 °C using RI detector. For the concentration of cordycepin by HPLC (Agilent, USA), methanol/distilled water (15:85, v/v) was used as a mobile phase. The elution was performed at a flow rate of 1.0 mL min^{-1} on HiQSil C18HS column (300 mm × 4.6 mm, 5 μm) at 40 °C using UV detector with the wavelength of 260 nm.

3. Results and discussion

3.1. GEM reconstruction for C. militaris

Aiming for simulating phenotypic growth behavior and cordycepin production, the *i*NR1329 extensively covers the primary metabolism for carbon catabolism, nitrogen utilization, as well as overall anabolic pathways towards metabolic precursors for *C. militaris* biomass and cordycepin productions (Figs. 1 and 2, Table 1). As a result, the *i*NR1329 included a total of 1329 genes and 1821 biochemical reactions that governed 1171 metabolites amongst four compartments i.e. cytosol, mitochondria, peroxisome and extracellular space (Fig. 1). The present model encompassed the central metabolic pathways, such as the glycolysis, the pentose phosphate pathway, the tricarboxylic acid cycle, as well as, the complete set of anabolic pathways involved in biosynthesis of amino acids, lipids, nucleotides, vitamins and cofactors. In addition, an electron transport chain associated with the genes encoding ubiquinone oxidoreductase (EC: 1.6.5.3), electron-transferring-flavoprotein dehydrogenase (EC: 1.5.5.1) and proton transporting two-sector ATPase (EC: 7.1.2.2) were also included into *i*NR1329. This finding suggests a conserved metabolism for the efficiency of ATP production by mitochondrial oxidative phosphorylation of *C. militaris* in response to high-altitude environment [29,30]. A unique pathway for cordycepin biosynthesis in *C. militaris* by several genes i.e. CCM_04436, CCM_04437 and CCM_04438 encoding for cordycepin synthetase complex was also reconstructed in *i*NR1329. In addition, overall stoichiometries of metabolic precursors involving in biomass synthesis reaction included in *i*NR1329 were quantitatively estimated based on macromolecular contents of carbohydrate, protein, lipid, nucleotide and vitamin obtained from our experimentation and literature (Fig. 2A).

3.2. Comparison of iNR1329 and an earlier metabolic network (iWV1170) of C. militaris

In a comparison between *i*NR1329 and an earlier metabolic network (*i*WV1170) of *C. militaris* [26], 363 genes were uniquely identified in *i*NR1329 and 966 genes were commonly identified (Tables 1 and S2). Accordingly, the *i*NR1329 was expanded a number of 435 unique metabolites as well as a number of 259 unique EC numbers (Tables 1, S3 and S4). Of these unique EC numbers, interestingly the cysteine and methionine metabolism (14 EC numbers), glycerophospholipid biosynthesis (9 EC numbers), folate biosynthesis (8 EC numbers), steroid biosynthesis (6 EC numbers), mannitol metabolism (6 EC numbers), sulfur metabolism (5 EC numbers), histidine metabolism (5 EC numbers), branched chain amino acids metabolism (4 EC numbers), glycan biosynthesis (4 EC numbers), galactose metabolism (3 EC numbers), and pentose phosphate pathway (3 EC numbers) were majorly identified

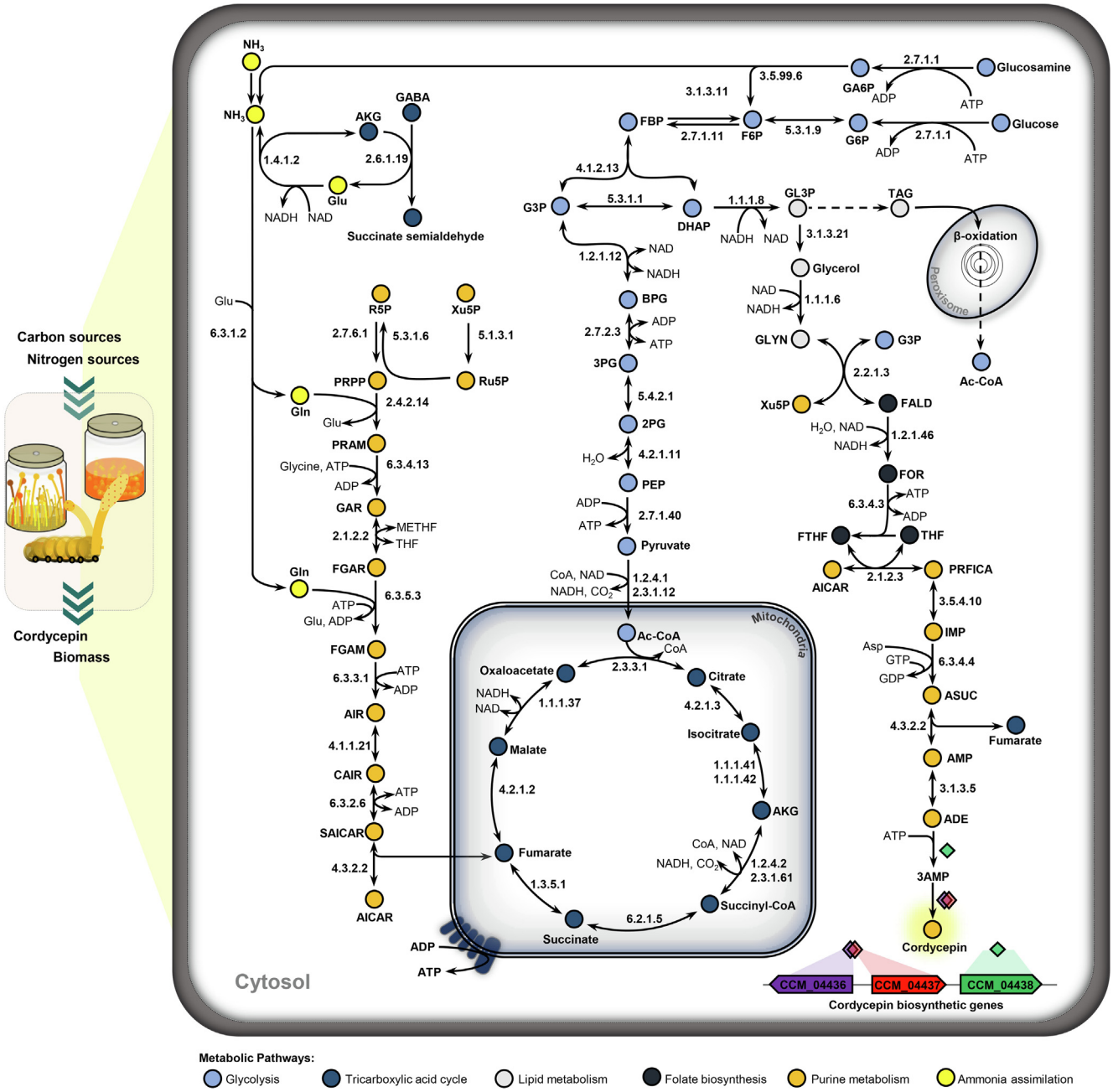

Fig. 1. A highlight metabolic landscape of *C. militaris* for growth and cordycepin production. Abbreviated metabolite names are as follows: NH_3, Ammonia; GABA, gamma-aminobutyrate; Glu, glutamate; AKG, 2-oxoglutarate; Gln, glutamine; R5P, ribose 5-phosphate; Xu5P, xylulose 5-phosphate; Ru5P, ribulose 5-phosphate; PRPP, 5-phospho-alpha-ribose 1-diphosphate; PRAM, 5-phospho-ribosylamine; GAR, 5-phospho-ribosyl-glycinamide; THF, tetrahydrofolate; METHF, 5,10-methenyltetrahydrofolate; FALD, formaldehyde; FTHF, 10-formyltetrahydrofolate; FOR, formate; FGAR, n(2)-formyl-n(1)-(5-phospho-ribosyl)glycinamide; FGAM, 2-formamido-n(1)-(5-phospho-ribosyl) acetamidine; AIR, 5-amino-1-(5-phospho-ribosyl) imidazole; AICAR, 5-amino-1-(5-phospho-ribosyl)imidazole-4-carboxamide; ADE, adenosine; PRFICA, 5-formamido-1-(5-phospho-ribosyl) imidazole-4-carboxamide; Ac-CoA, acetyl-CoA; CAIR, 1-(5-phospho-ribosyl)-5-amino-4-imidazolecarboxylate; PEP, phosphoenolpyruvate; ASUC, adenylosuccinate; IMP, inosine monophosphate; FBP, beta-fructose 1,6-bisphosphate; 2PG, 2-phospho-glycerate; 3PG, 3-phospho-glycerate; GL3P, glycerol 3-phosphate; G3P, glyceraldehyde 3-phosphate; BPG, 3-phospho-glyceroyl phosphate; G6P, glucose 6-phosphate; GLYN, glycerone; DHAP, glycerone phosphate; F6P, beta-fructose 6-phosphate; GA6P, glucosamine 6-phosphate; Asp, aspartate; 3AMP, adenosine-3′-monophosphate; AMP, adenosine-5′-monophosphate; ADP, adenosine-5′-diphosphate; ATP, adenosine-5′-triphosphate; NAD, nicotinamide adenine dinucleotide; NADH, reduced nicotinamide adenine dinucleotide; SAICAR, (5-amino-1-(5-phospho-ribosyl)imidazole-4-carboxamido) succinic acid; GDP, guanosine-5′-diphosphate; GTP, guanosine-5′-triphosphate and TAG, triacylglycerol.

(Fig. 2B). In addition, the other unique EC numbers were found to be involved in the conversion of different hormones, such as serotonin, adrenaline and dopamine towards amino acids production (Table S3). The inclusion of hormone catalysis could be matched with the natural behavior of *C. militaris* which almost assimilates nitrogen and carbon sources from larva corpus that included mostly juvenile hormones (e.g. serotonin and dopamine) [31]. For the other unique reactions, such as 17 spontaneous reactions, 267 transport reactions between intracellular compartments, i.e. cytosol, mitochondria and peroxisome, as well as environment are identified as shown in Table 1.

3.3. Quantitative determination of iNR1329 for growth capability

The model capability of *i*NR1329 was quantitatively assessed by predicting growth rates of *C. militaris* on different carbon sources

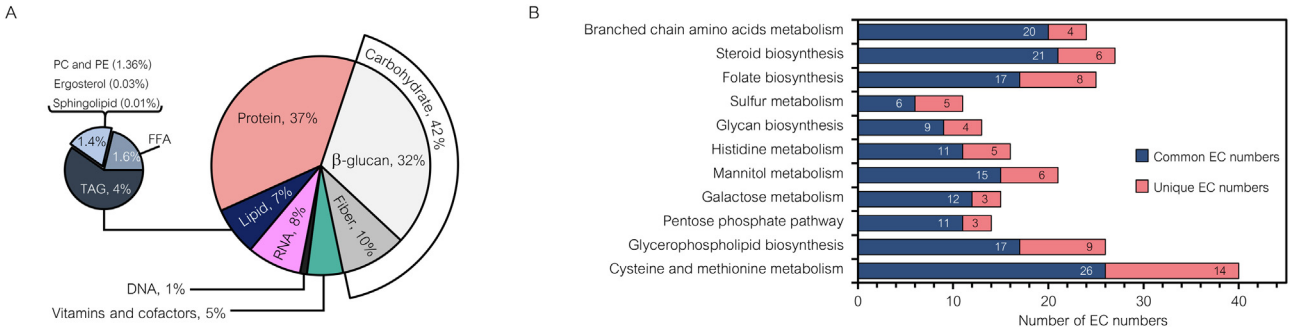

Fig. 2. GEM features of *C. militaris* in context of biomass and identified EC numbers. (A) Metabolic precursors involving in biomass synthesis. (B) Number of common and unique EC numbers identified in *i*NR1329. Abbreviated metabolites are as follows: PC, phosphatidylcholine; PE, phosphatidylethanolamine; FFA, free fatty acid; TAG, triacylglycerol; DNA, deoxyribonucleic acid and RNA, ribonucleic acid.

Table 1
Comparative characteristics of genome-scale metabolic networks for *C. militaris*.

Characteristics	*i*WV1170[a]	*i*NR1329 (This study)
Total genes	9561	9561
Included genes (unique/common)	1170 (204/966)	1329 (363/966)
Total metabolites (unique/common)	894 (158/736)	1171 (435/736)
Total biochemical reactions	1267	1821
Enzymatic reactions	1250	1391
• EC numbers (unique/common)	679 (11/668)	927 (259/668)
Non-enzymatic reactions	17	430
• Spontaneous reactions (unique/common)	13 (9/4)	21 (17/4)
• Transport reactions (unique/common)	4 (–/4)	271 (267/4)
• Exchange reactions	–	137
-In-out	–	135
-Excretion of biomass and cordycepin	–	2
• Biomass synthesis reaction	–	1

[a] Network data was taken from Vongsangnak et al. [26].

under aerobic condition (Table 2). It was found that the predictive growth rates agreed well with the experimental data with error rates < 5% (Table 2). Observably, *C. militaris* yielded the highest growth rate on sucrose with μ_{max} of 0.0114 ± 0.0014 h^{-1} following by glucose (0.0100 ± 0.0027 h^{-1}) and fructose (0.0098 ± 0.0018 h^{-1}). Significant reductions in growth were observed on xylose and arabinose with μ_{max} ranged between 0.0022 and 0.0051 h^{-1}, respectively. These experimental results clearly demonstrated that xylose and arabinose were less favored to *C. militaris* growth which were in agreement with earlier studies [15,16,32]. Considering growth prediction on arabinose or xylose using model simulation, *i*NR1329 suggests that the pentose sugars were metabolized through pentose and glucuronate interconversions and then phosphorylated by xylulose 5-phosphotransferase (EC: 2.7.1.17) to generate xylulose 5-phosphate as a metabolic precursor towards the oxidative pentose phosphate pathway. This specific utilization pathway resulted in an increased ATP cost which may cause slow growth.

3.4. Cellular growth assessment under nutritional perturbation using *i*NR1329

Considering on nutrients for *C. militaris* growth, *i*NR1329 was further simulated under the different nutritional environments, for example, in carbon and nitrogen limited condition (CN-limited condition). We observed that *i*NR1329 could utilize a wide range of carbon and nitrogen containing substrates under CN-limited condition, such as chitin, glucosamine, gamma-aminobutyrate (GABA), and some amino acids as a complex source of carbon and nitrogen for thriving growth (Fig. 3, Cluster 1). Not surprisingly, chitin and its derivatives are major components of insect exoskeleton which is the direct source of nutrient for *C. militaris* in nature [3]. In addition, GABA could also be consumed in the model as an alternative source of carbon and nitrogen. This is consistent with the fact that rice grain is a source of GABA which supports *C. militaris* growth in artificial cultivation. *C. militaris* can utilize some other amino acids as alternative sources of carbon

Table 2
Quantitative comparison between the maximum specific growth rates (μ_{max}, h^{-1}) obtained from experimentation and *i*NR1329 prediction on different carbon sources.

Carbon source	Uptake rate (mmol $gDW^{-1}h^{-1}$)	Extracellular cordycepin production (g L^{-1})	Growth rate, μ_{max} (h^{-1})		Error rate (%)
			Experiments[a]	Prediction[a]	
Glucose	0.1448 ± 0.0872	0.1090 ± 0.0124	0.0100 ± 0.0027	0.0100	0.40
Fructose	0.1472 ± 0.0042	0.0583 ± 0.0045	0.0098 ± 0.0018	0.0103	4.65
Arabinose	0.1074 ± 0.0051	0.0203 ± 0.0021	0.0051 ± 0.0007	0.0051	0.56
Xylose	0.0681 ± 0.0038	0.0257 ± 0.0016	0.0022 ± 0.0012	0.0021	3.24
Sucrose	0.0815 ± 0.0250	0.0835 ± 0.0100	0.0114 ± 0.0014	0.0117	2.42

[a] The growth physiology from experimentation and *in silico* growth prediction were carried out in defined media used ammonia as a sole nitrogen source.

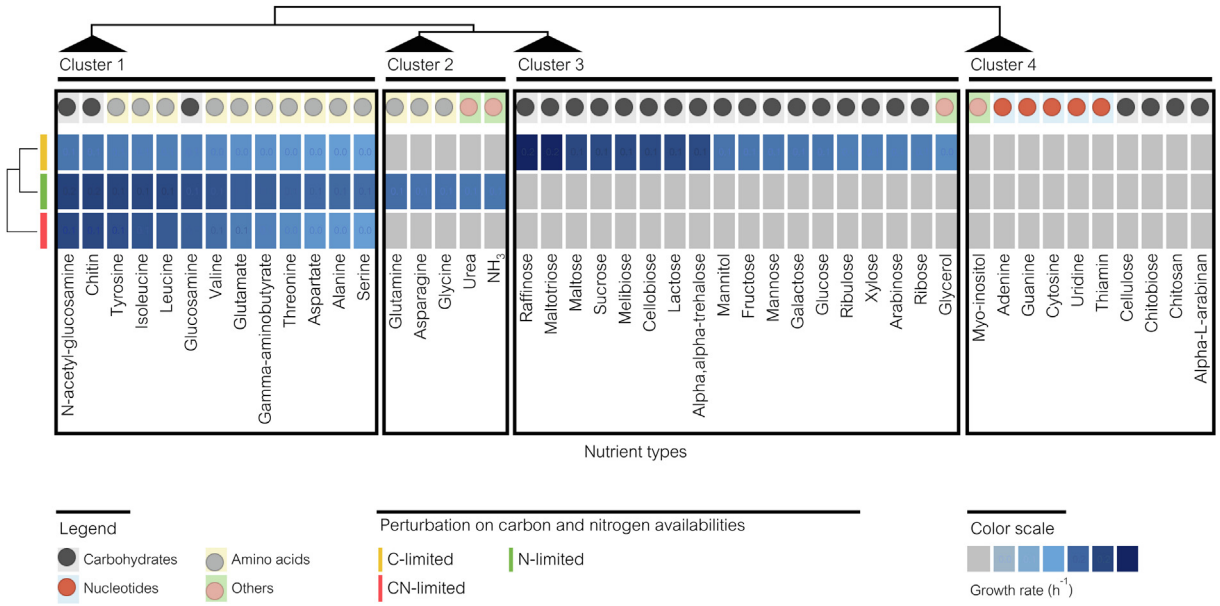

Fig. 3. Growth capability of *C. militaris* underlying nutritional perturbation. A heatmap represents the prediction growth rates governed under the perturbation on nutrient variation of 46 different nutrient types under carbon limited condition (C-limited), nitrogen limited condition (N-limited) and CN-limited condition. Table S5 shows all details for prediction growth rates governed under the perturbation on the other remaining nutrient types.

and nitrogen, such as glutamate, aspartate, isoleucine, and serine (Fig. 3, Cluster 1), however *i*NR1329 could utilize glutamine, asparagine, glycine, urea and ammonia as single sources of nitrogen (Fig. 3, Cluster 2). Observably, *i*NR1329 could utilize glucose, sucrose or xylose as examples of single carbon sources (Fig. 3, Cluster 3). This is in agreement with earlier reports from Raethong et al. (2018) [15] and Wongsa et al. (2019) [16]. Notably, the *i*NR1329 could not utilize cellulose as sole carbon source (Fig. 3, Cluster 4) which is in agreement with an earlier experimental verification by Shang et al. (2016) [32].

3.5. In silico analysis of ammonia metabolism using iNR1329

C. militaris has evolved multiple enzymes and transporters to access diverse nutrients from insect hosts [32], however the metabolic behavior of this fungus in response to nutritional variation remains largely unknown. We thus compared metabolic flux distributions in different nutrient types via FBA using *i*NR1329. The results suggested that *C. militaris* could utilize various nutrients and redirect them through the ammonia metabolism (Fig. 4). For example, glucosamine appears to be catalyzed by chitinolytic

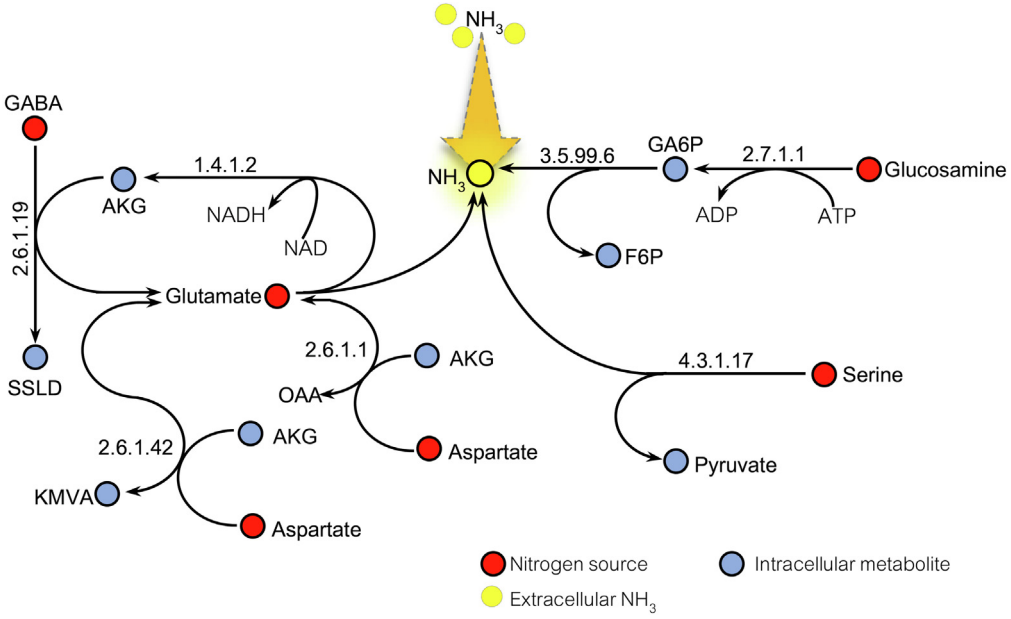

Fig. 4. Subnetwork of ammonia metabolism in *C. militaris*. Abbreviated metabolites are as follows: NH_3, ammonia; GABA, gamma-aminobutyrate; AKG, 2-oxoglutarate; OAA, oxaloacetate; KMVA, 3-methyl-2-oxopentanoic acid; GA6P, glucosamine 6-phosphate; SSLD, succinate semialdehyde; F6P, beta-fructose 6-phosphate; ADP, adenosine-5′-diphosphate; ATP, adenosine-5′-triphosphate; NAD, nicotinamide adenine dinucleotide and NADH, reduced nicotinamide adenine dinucleotide.

Table 3
Experimental validation of the POPCORN-based rational design of synthetic media for fast growth and cordycepin overproduction in *C. militaris*.

Experimental growth characteristics	C:N ratio			
	0.5:1	1:1	8:1	100:1
Growth rate, μ_{max} (h^{-1})	0.0112 ± 0.0015	0.0110 ± 0.0006	0.0174 ± 0.0031	0.0110 ± 0.0027
Biomass production (gDW L^{-1})	2.1197 ± 0.2487	4.1048 ± 0.3849	6.0919 ± 0.5289	3.8224 ± 0.3501
Biomass productivity (gDW $L^{-1}h^{-1}$)	0.0087 ± 0.0012	0.0074 ± 0.0005	0.0091 ± 0.0021	0.0076 ± 0.0004
Extracellular cordycepin production (g L^{-1})	0.1869 ± 0.0349	0.2120 ± 0.0052	0.3776 ± 0.0055	0.0657 ± 0.0055
Extracellular cordycepin productivity (mg $L^{-1}h^{-1}$)	0.4323 ± 0.0470	0.2360 ± 0.0906	0.5430 ± 0.0675	0.0716 ± 0.0572

activities of glucosamine 6-phosphotransferase (EC: 2.7.1.1) and glucosamine 6-phosphate aminohydrolase (EC: 3.5.99.6) to supply fructose 6-phosphate and ammonia into central metabolism. Moreover, the transamination of GABA via 4-aminobutyrate-2-oxoglutarate transaminase (EC: 2.6.1.19) together with deamination by glutamate oxidoreductase (EC: 1.4.1.2) to channel 2-oxoglutarate and ammonia into the central metabolism. In addition to glutamate, deamination of serine by serine ammonia lyase (EC: 4.3.1.17) also yielded pyruvate and ammonia to feed the central metabolism. Given its pivotal role in nitrogen metabolism, ammonia appeared to be a preferred complementary nutrient with other carbon sources in relieving the metabolic burden for nitrogen source (Fig. 3, Cluster 3). This achieved result is supported by earlier reports where ammonium phosphate and ammonium sulphate were used as the best nitrogen sources for the *in vitro* growth of *C. militaris* with average DW of 167.53 mg and 163.22 mg, respectively [33]. Besides, ammonia with a suitable concentration was significantly increased the production of extracellular cordycepin up to 420 mg L^{-1} in shake flask culture [34].

3.6. POPCORN-based rational design of synthetic media for optimizing *C. militaris* growth and cordycepin overproduction

Among the preferred carbon source, glucose was found for obtaining the highest extracellular cordycepin production at 0.10 90 ± 0.0124 g L^{-1} (Table 2). Previous work reported that while glucose was used as a carbon source, the production of cordycepin could be increased by allocated the concentration of nitrogen source in the cultivation media [35]. The growth and cordycepin production were shown to be tightly correlated to the carbon/nitrogen ratio (C:N ratio) [35,36]. Thus, an appropriation of C:N ratio would be critical and straightforward application for rational design of synthetic media for optimizing *C. militaris* cultivation. To do this, we developed a constraint-based modeling method to determine the PrOPortion of CarbOn and nitRogeN (POPCORN) of the synthetic media for optimizing growth and cordycepin overproduction in *C. militaris*. This method was implemented as a MATLAB function that generates a series of C:N ratios ranged from low to high for model simulation with FBA. As plotted in Fig. 5, the simulation results showed that μ_{max} was gradually increased along with the increase of C:N ratio and reached the highest μ_{max} at C:N ratio of 12.7:1. After this point, the μ_{max} was obviously decreased suggesting that the C:N ratio of 12.7:1 is optimal for *C. militaris* growth. This optimal C:N ratio was remarkably closed to the optimal C:N ratio of 12:1 of a semi-synthetic medium designed for the mycelial growth of *Cordyceps sinensis* [37]. Furthermore, the simulation results also showed the raised of cordycepin production flux in parallel with μ_{max} where the highest production flux and the yield of cordycepin on biomass were achieved at the C:N ratio of 8.3:1 (Fig. 5). This simulation results were validated by cultivation series of *C. militaris* on the 4 rational synthetic media (Table S1). As shown in Table 3, the synthetic media with the C:N ratio of 8:1 yielded the fastest growth rate at 0.0174 ± 0.0031 h^{-1} and successfully improved from 0.1090 ± 0.0124 g L^{-1} (Table 2) to 0.3776 ± 0.0055 g L^{-1} (Table 3) with accounting for 3.5-fold increase in cordycepin production.

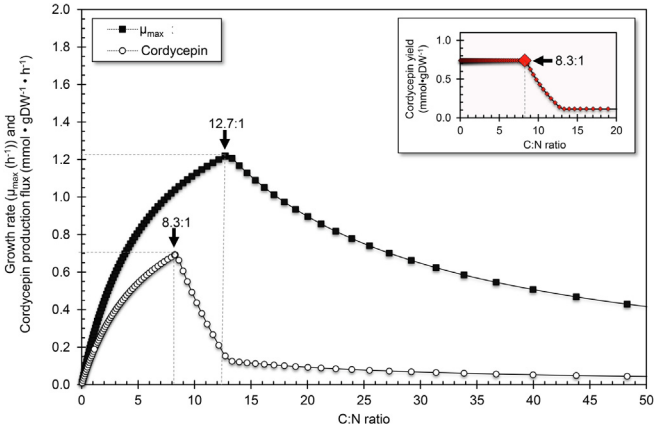

Fig. 5. POPCORN-based rational design of synthetic media for fast growth and cordycepin overproduction in *C. militaris*. The μ_{max}, cordycepin production flux and the yield of cordycepin on biomass are plotted against a series of different C:N ratios.

4. Conclusions

We presented *i*NR1329, the first GEM of *C. militaris*, and validated its performance with the batch cultivation experiments in different carbon sources. The *in silico* growth predictions of *i*NR1329 were in good agreement with the observed experimental results. The simulated flux distributions under nutritional perturbation of *i*NR1329 highlighted that the utilization of ammonia as a sole nitrogen source is preferably for supporting growth capability of *C. militaris*. Particularly, glucose was experimentally observed as the most favorable carbon source for cordycepin production. Therefore, we developed the POPCORN approach for rational designing of synthetic media composition for optimizing growth and cordycepin production in *C. militaris*. Through determining the optimum proportion of glucose and ammonia, this optimized synthetic media significantly increased the growth rate of *C. militaris* and successfully improved cordycepin production. Our results not only demonstrated the high quality of *i*NR1329, but also validated a novel approach of rational design of media composition for metabolic engineering purposes.

Declaration of Competing Interest

The authors declare that they have no known competing financial interests or personal relationships that could have appeared to influence the work reported in this paper.

Acknowledgements

The authors would like to thank The Thailand Research Fund (RSA6180001) and Interdisciplinary Graduate Program in Bio-

science, Faculty of Science, Kasetsart University for financial supports, Department of Zoology, Faculty of Science, Kasetsart University for laboratory facilities and Department of Biology and Biological Engineering, Chalmers University of Technology, Sweden for computing facilities and resources. This research was supported from graduate scholarship provided by the National Research Council of Thailand (NRCT) as of fiscal year 2018. NR gratefully acknowledges funding supports from Science Achievement Scholarship of Thailand (SAST) and the International Affairs Division (IAD) at Kasetsart University. WV would like to thank Omics Center for Agriculture, Bioresources, Food, and Health, Kasetsart University (OmiKU) and Talented Young Scientist Program (TYSP), China (Grant ID: Thailand-18-005) for funding supports.

Author contributions

NR performed the experiments, carried out the simulations, analyzed the results and wrote the manuscript. HW and NR performed the reconstruction. HW, JN and WV assisted the modeling and simulation. HW, JN, NR and WV revised the manuscript. WV conceived and designed throughout the studies, analyzed and interpreted all the achieved results. All authors reviewed and approved the final manuscript.

Appendix A. Supplementary data

Supplementary data to this article can be found online at https://doi.org/10.1016/j.csbj.2019.11.003.

References

[1] Adnani N, Chevrette MG, Adibhatla SN, Zhang F, Yu Q, et al. Coculture of marine invertebrate-associated bacteria and interdisciplinary technologies enable biosynthesis and discovery of a new antibiotic, Keyicin. ACS Chem Biol 2017;12:3093–102.
[2] Zipperer A, Konnerth MC, Laux C, Berscheid A, Janek D, et al. Human commensals producing a novel antibiotic impair pathogen colonization. Nature 2016;535:511.
[3] Cui JD. Biotechnological production and applications of *Cordyceps militaris*, a valued traditional Chinese medicine. Crit Rev Biotechnol 2015;35:475–84.
[4] Molnár I, Gibson DM, Krasnoff SB. Secondary metabolites from entomopathogenic Hypocrealean fungi. Nat Prod Rep 2010;27:1241–75.
[5] Wang B, Kang Q, Lu Y, Bai L, Wang C. Unveiling the biosynthetic puzzle of destruxins in *Metarhizium* species. Proc Natl Acad Sci U S A 2012;109:1287–92.
[6] Wei G, Lai Y, Wang G, Chen H, Li F, et al. Insect pathogenic fungus interacts with the gut microbiota to accelerate mosquito mortality. Proc Natl Acad Sci U S A 2017;114:5994–9.
[7] Yoon SY, Park SJ, Park YJ. The anticancer properties of cordycepin and their underlying mechanisms. Int J Mol Sci 2018;19:3027.
[8] Cui ZY, Park SJ, Jo E, Hwang I-H, Lee K-B, et al. Cordycepin induces apoptosis of human ovarian cancer cells by inhibiting CCL5-mediated Akt/NF-κB signaling pathway. Cell Death Discov 2018;4:62.
[9] Huang CY, Fong YC, Lee CY, Chen MY, Tsai HC, et al. CCL5 increases lung cancer migration via PI3K, Akt and NF-κB pathways. Biochem Pharmacol 2009;77:794–803.
[10] Qi G, Zhou Y, Zhang X, Yu J, Li X, et al. Cordycepin promotes browning of white adipose tissue through an AMP-activated protein kinase (AMPK)-dependent pathway. Acta Pharm Sin B 2019;9:135–43.
[11] Das SK, Masuda M, Sakurai A, Sakakibara M. Medicinal uses of the mushroom *Cordyceps militaris*: current state and prospects. Fitoterapia 2010;81:961–8.
[12] Peng Z, Xia Y, Xiao G, Xiong C, Hu X, et al. Genome sequence of the insect pathogenic fungus *Cordyceps militaris*, a valued traditional Chinese medicine. Genome Biol 2011;12:R116.
[13] Chen Y, Wu Y, Liu L, Feng J, Zhang T, et al. Study of the whole genome, methylome and transcriptome of *Cordyceps militaris*. Sci Rep 2019;9:898.
[14] Kramer GJ, Nodwell JR. Chromosome level assembly and secondary metabolite potential of the parasitic fungus *Cordyceps militaris*. BMC Genomics 2017;18:912.
[15] Raethong N, Laoteng K, Vongsangnak W. Uncovering global metabolic response to cordycepin production in *Cordyceps militaris* through transcriptome and genome-scale network-driven analysis. Sci Rep 2018;8:9250.
[16] Wongsa B, Raethong N, Chumnanpuen P, Wong-ekkabut J, Laoteng K, et al. (2019) Alternative metabolic routes in channeling xylose to cordycepin production of *Cordyceps militaris* identified by comparative transcriptome analysis. Genomics. In press.
[17] Nielsen J, Keasling JD. Engineering cellular metabolism. Cell 2016;164:1185–97.
[18] O'Brien EJ, Monk JM, Palsson BO. Using genome-scale models to predict biological capabilities. Cell 2015;161:971–87.
[19] Wang H, Marcišauskas S, Sánchez BJ, Domenzain I, Hermansson D, et al. RAVEN 2.0: A versatile toolbox for metabolic network reconstruction and a case study on *Streptomyces coelicolor*. PLoS Comput Biol 2018;14:e1006541.
[20] Agren R, Liu L, Shoaie S, Vongsangnak W, Nookaew I, et al. The RAVEN toolbox and its use for generating a genome-scale metabolic model for *Penicillium chrysogenum*. PLoS Comput Biol 2013;9:e1002980.
[21] David H, Ozcelik IS, Hofmann G, Nielsen J. Analysis of *Aspergillus nidulans* metabolism at the genome-scale. BMC Genomics 2008;9:163.
[22] Vongsangnak W, Olsen P, Hansen K, Krogsgaard S, Nielsen J. Improved annotation through genome-scale metabolic modeling of *Aspergillus oryzae*. BMC Genomics 2008;9:245.
[23] Dreyfuss JM, Zucker JD, Hood HM, Ocasio LR, Sachs MS, et al. Reconstruction and validation of a genome-scale metabolic model for the filamentous fungus *Neurospora crassa* using FARM. PLoS Comput Biol 2013;9:e1003126.
[24] Caspi R, Billington R, Fulcher CA, Keseler IM, Kothari A, et al. The MetaCyc database of metabolic pathways and enzymes. Nucleic Acids Res. 2017;46:D633–9.
[25] Kanehisa M, Sato Y, Kawashima M, Furumichi M, Tanabe M. KEGG as a reference resource for gene and protein annotation. Nucleic Acids Res 2016;44:D457–62.
[26] Vongsangnak W, Raethong N, Mujchariyakul W, Nguyen NN, Leong HW, et al. Genome-scale metabolic network of *Cordyceps militaris* useful for comparative analysis of entomopathogenic fungi. Gene 2017;626:132–9.
[27] Mi JN, Wang JR, Jiang ZH. Quantitative profiling of sphingolipids in wild *Cordyceps* and its mycelia by using UHPLC-MS. Sci Rep 2016;6:20870.
[28] Hwang SW. Long-term preservation of fungus cultures with liquid nitrogen refrigeration. Appl Microbiol 1966;14:784–8.
[29] Sung GH. Complete mitochondrial DNA genome of the medicinal mushroom *Cordyceps militaris* (Ascomycota, Cordycipitaceae). Mitochondrial DNA 2015;26:789–90.
[30] Luo Y, Yang X, Gao Y. Mitochondrial DNA response to high altitude: a new perspective on high-altitude adaptation. Mitochondrial DNA 2013;24:313–9.
[31] Zhang Q, Lu YX, Xu WH. Proteomic and metabolomic profiles of larval hemolymph associated with diapause in the cotton bollworm, *Helicoverpa armigera*. BMC Genomics 2013;14:751.
[32] Shang Y, Xiao G, Peng Z, Cen K, Zhan S, et al. Divergent and convergent evolution of fungal pathogenicity. Genome Biol Evol 2016;8:1374–87.
[33] Sehgal A, Sagar A. *In vitro* isolation and influence of nutritional conditions on the mycelial growth of the entomopathogenic and medicinal fungus *Cordyceps militaris*. Plant Pathol J 2006;5:315–21.
[34] Mao XB, Zhong JJ. Significant effect of NH_4^+ on cordycepin production by submerged cultivation of medicinal mushroom *Cordyceps militaris*. Enzyme Microb Technol 2006;38:343–50.
[35] Mao XB, Eksriwong T, Chauvatcharin S, Zhong JJ. Optimization of carbon source and carbon/nitrogen ratio for cordycepin production by submerged cultivation of medicinal mushroom *Cordyceps militaris*. Process Biochem 2005;40:1667–72.
[36] Park JP, Kim SW, Hwang HJ, Yun JW. Optimization of submerged culture conditions for the mycelial growth and exo-biopolymer production by *Cordyceps militaris*. Lett Appl Microbiol 2001;33:76–81.
[37] Dong CH, Yao YJ. Nutritional requirements of mycelial growth of *Cordyceps sinensis* in submerged culture. J Appl Microbiol 2005;99:483–92.